PACS numbers: 77.84.LF doi: 10.15407/Surface.2023.15.200

CRYSTALLINE POTASSIUM DIHYDROGEN PHOSPHATE (KDP) POWDERS

An.D. Zolotarenko [1,2], Ol.D. Zolotarenko [1,2], Z.A. Matysina[1], N.A. Shvachko[1,3], N.Y. Akhanova [4,5], M. Ualkhanova [5], D.V. Shchur [1,6], M.T. Gabdullin [4], Yu.I. Zhirko[6], A.D. Zolotarenko [1], E.P. Rudakova [1,2], M.V. Chymbai [1,2], Yu.O. Tarasenko [2], O.O. Havryliuk [2]

[1] Frantsevich Institute for Problems of Materials Science of N.A.S. of Ukraine, 3, Krzhizhanovskogo Str., 03142,Kyiv, Ukraine * A.D.Zolotarenko@gmail.com
[2] Chuiko Institute of Surface Chemistry, of the N.A.S. of Ukraine, 17 General Naumov Str., 03164, Kyiv, Ukraine.
[3] Kyiv National University of Construction and Architecture, 31, Povitroflotskyi Avenue., Kyiv, 03037, Ukraine.
[4] Kazakhstan-British Technical University, 59, Tole bi Str., 050000, Almaty, Kazakhstan
[5] Al-Farabi Kazakh National University, Al-Farabi, 71, 050040, Almaty, Kazakhstan.
[6] The Institute of Applied Physics, Nat. Acad. of Sci. of Ukraine,58, Petropavlivska Str., Sumy 40000, Ukraine.

The article discusses the use of KDP ferroelectric crystals (phosphates and arsenates of potassium, rubidium, cesium) and their deuterated analogues in various industries, including the creation of electro-optical devices and as hydrogen sorbents. The paper describes the physical properties of KDP crystals, changes in their properties near the phase transition temperature, as well as methods for obtaining KDP nanocrystals and their application in biomedicine.

The paper also states that the phase transition in KDP crystals occurs near room temperature and manifests itself in a change in their physical properties, such as dielectric constant, optical properties, and heat capacity. In addition, approaching the phase transition temperature causes a change in the crystal lattice parameters, which can lead to the appearance of anomalous effects.

The structure of the unit cell of potassium dihydrogen phosphate (KH_2PO_4) is considered. The plots of the temperature dependence of the order parameter of spontaneous polarization and the plots of the temperature dependence of the configurational heat capacity of the crystal in the phase transition region are calculated, and the plots of the temperature of the inverse and direct dielectric susceptibility are calculated. Graphs of the order parameter, which characterizes the degree of spontaneous polarization for different temperatures, depending on the strength of the external electric field, are also calculated.

Keywords: *KDP crystals, thermodynamic theory, ferroelectrics, hydrogen sorbents, molecular-kinetic representations, order, Curie-Weiss law.*

Introduction

KDP (crystalline potassium dihydrogen phosphate) is one of the most common ferroelectrics (KH_2PO_4, RbH_2PO_4, CsH_2PO_4, KH_2AsO_4, RbH_2AsO_4, CsH_2AsO_4). It is used in various electronic devices, such as lasers, sensors and transformers. There are several methods for obtaining KDP nanocrystals, including mechanical grinding, hydrothermal synthesis, and supercritical slurry methods.

KDP (potassium diethyl phosphate) is a common representative of ferroelectrics. The main properties of KDP are related to its crystal structure, which exhibits the effect of

ferroelectricity under certain conditions. Ferroelectric materials have the ability to change their polarization in response to mechanical stress or temperature changes. In addition, KDP has a high second harmonic, which makes it useful for creating second harmonic devices. KDP crystals are also well studied in the field of nonlinear optics and are used as a material for creating quantum generators and detectors.

KDP has a number of advantages over other materials such as high second harmonic, high optical non-linearity, high electro-optical constant and high thermal stability. In addition, KDP is a relatively cheap material and can be grown in large volumes. In this regard, KDP is widely used in various applications such as electronics, laser technology, optical communications, acoustics, medicine and others. For example, KDP is used as a material for creating crystal oscillators, piezoelectric transducers (sensors), acousto-optic modulators, etc.

KDP crystals is mixed uniaxial crystals (ferroelectrics, ferroelastics and simultaneously pyroelectrics and pyroelastics). The physical properties of KDP crystals are simpler than those of other ferroelectrics. They have only one phase transition from the para- to the ferrophase, they have only one axis of spontaneous polarization and deformation. The temperatures of phase transitions to the polarized and spontaneously deformed phases coincide. In this case, the phase transition occurs at the same temperature with its increase or decrease, i.e. no temperature hysteresis.

KDP nanocrystals and carbon nanostructures (fullerenes [1–4], fullerites [5], endofullerins [6], graphenes [7–8], nanotubes [9–10]) with various synthesis methods [11–19] can be used as fillers for creating new composites [20–23] suitable for 3D printing technology [24–27].

In addition, KDP structures [28], as well as many other nanofillers [29–34], can be used in the biomedical field, provided that they are nanosized. Such structures can also be used as promising sorbents [35–43], for example, hydrogen sorbents, both in the form of carbon nanostructures [44–48], metals and various alloys [49–66]. All this will complement the existing developments in the field of hydrogen energy [67-73]. Of course, the main role in the properties of a nanomaterial is played by the type of system, which can be single-component [74–75] or multicomponent [76–79]. No less important is the technology of preparation [80-85] and processing of the material before its use, which confirms the theoretical [90-92] and experimental [93-100] data.

Thus, the study of KDP crystals is of scientific and practical interest.

The physical properties of KDP crystals undergo special changes [101–122] in the vicinity of the phase transition temperature (Fig. 1), which manifest themselves as the appearance of sharp peaks, kinks, bends, and jumps. KPD crystals are characterized by the following properties:

I. The degree of their spontaneous polarization P along the *c* axis of the crystal decreases with increasing temperature, at first gradually, and near the Curie temperature T_o, sharply but continuously [105, 111], i.e. the phase transition is a transition of the second order, close to the first (Fig. 1 (a)).

II. The presence of an external electric field or an oriented external mechanical stress increases the spontaneous polarization or deformation (Fig. 1(b)) [111], while the growth pattern depends on the crystal temperature.

III. The specific heat capacity C at the Curie point undergoes a typical change - a sharp peak-like growth (Fig. 1 (c, d)) [104, 106, 107, 115].

IV. The permittivity in the direction ε_c of the *c* axis increases sharply at the phase transition point (Fig. 1 (e)) [101, 102]. With a decrease in temperature at $T \rightarrow T_o$, the value of ε_c increases according to the hyperbolic law up to a value of 10^5, while the Curie-Weiss law is valid $\varepsilon_c \sim \frac{1}{T - T_o}$, and the inverse permittivity near the critical point above the Curie point increases

linearly with temperature [112]. The permittivity of ε_a in the direction perpendicular to the *c* axis is also high. Above T_0, the value of ε_a slightly increases with increasing temperature, and below the temperature T_0, it decreases.

V. The thermal conductivity coefficient η undergoes a kink at the phase transition point (Fig. 1 (e)) [113, 114]. However, it should be noted that the nature of the temperature dependence of the thermal conductivity coefficients of KDP crystals has not yet been fully studied.

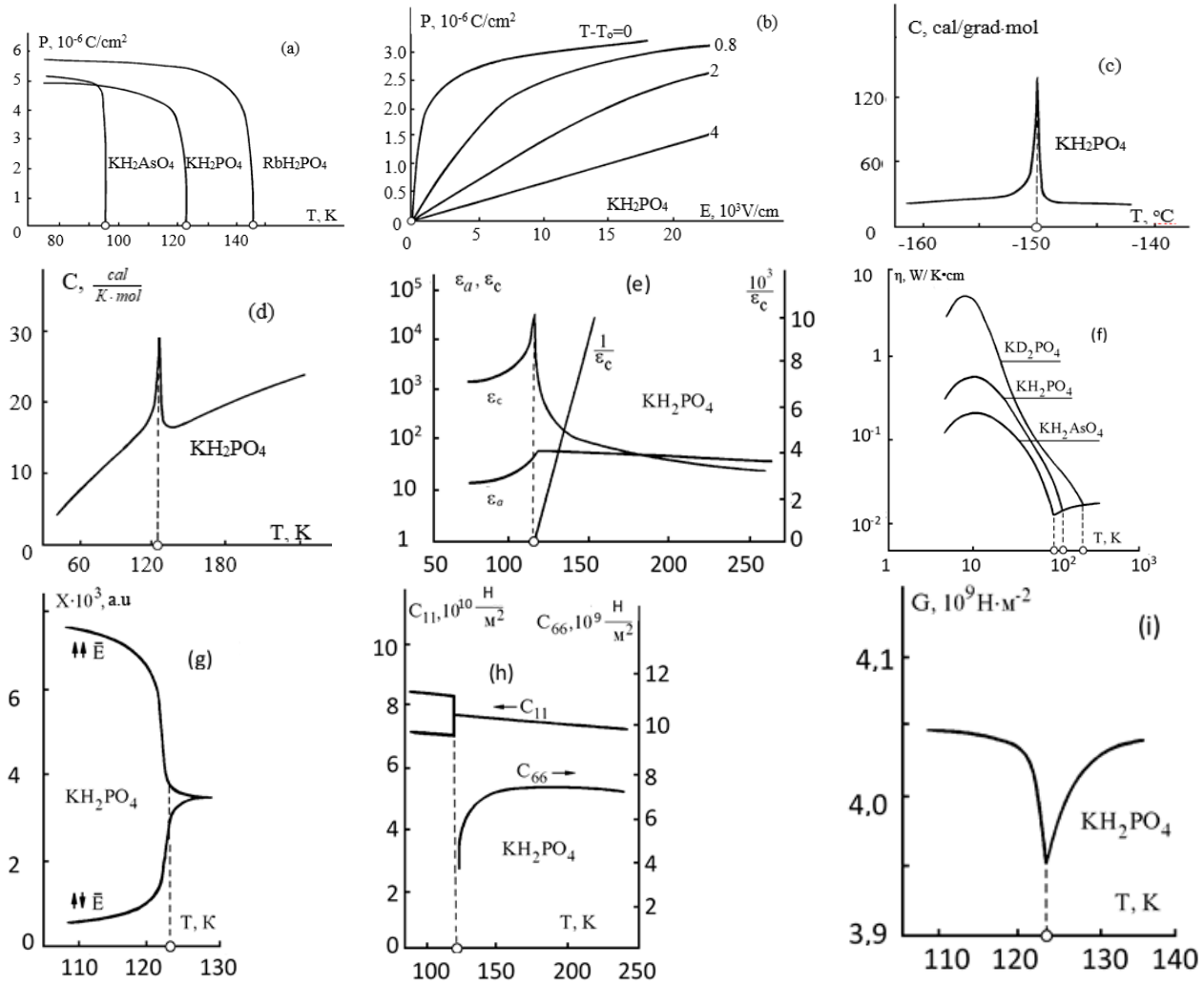

Fig. 1. Experimental graphs of the temperature dependence of spontaneous polarization P(T) (a), heat capacity C(T) (c, d), direct and reverse permittivity ε_c (T)(e), thermal conductivity coefficient η(T) (f) , spontaneous deformation X(T)(g), elastic constants cii(T)(h), shear modulus G(T) (i), as well as dependence of spontaneous polarization on electric field strength P(E) (b) KDP of crystals in the vicinity of the phase transition temperature (marked with circles on the abscissa axis of the curves (a)) paraelectric – ferroelectric

VI. Linear spontaneous strain X is a shear in a plane perpendicular to the c axis (Fig. 1(g)) [103]. The upper part of the curve in Fig. 1 (g) corresponds to the electric field strength E, parallel to the direction of polarization, the lower one corresponds to the field, which is strictly opposite to the direction of spontaneous polarization. At temperature T_0, the upper and lower parts of the curves converge, forming one curve.

VII. The elastic constant c_{11} at the Curie point T_0 undergoes a relatively weak change: there is a small abrupt increase and decrease for external electric fields directed along and

against the *c* axis, respectively (Fig. 1(h) [109]. The elastic constant c_{66} decreases with decreasing temperature near the Curie point drops to zero [108].

VIII. Модуль сдвига G в точке фазового перехода имеет аномалию в виде V-образного минимума (рис. 1 (i)) [118].

The physical properties of KDP crystals have already been described in many works [119–122]. In the same work, the thermodynamic theory of ferroelectrics of various structures, including KDP crystals, is presented.

The statistical theory of KDP crystals will be presented below, which makes it possible to determine, explain and substantiate the physical properties listed above, developed on the basis of molecular kinetic concepts. It has long been established that the phase transitions from the para- to the ferrophase of ferroelectrics and ferroelastics are transitions of the ordering type [103, 118-122].

It is of interest to determine the temperature dependence of the order parameter $\xi(T)$, which is proportional to the degree of spontaneous polarization and deformation, as well as to elucidate the conditions under which a phase transition in KDP crystals turns out to be a transformation of the second order, close to the first, to estimate the Curie temperature (T_0) of the phase transition, to establish dependence of the order parameter on the strength of the external electric field $\xi(E)$ or external oriented mechanical stress, the possibility of manifestation of features on the last dependencies, the evaluation of the configurational heat capacity, its temperature dependence C(T) and the jump at the phase transition point, the determination of the temperature dependences of the direct and inverse dielectric permeability ε or susceptibility χ ($\chi=1+\varepsilon$), checking the validity of the Curie-Weiss law for the value $1/\chi$ [123-125]. The answers to these questions are disclosed below in the text of the work.

Structure of kdp crystals. Order parameters

The structure of H_{22} potassium dihydrogen phosphate KH_2PO_4 was first studied by West [126] and refined in [127, 128]. According to West [126], the unit cell of a crystal in the paraphase is tetragonal with lattice parameters a = 7.434 Å, c = 6.945 Å (Fig. 2(a)). Fraser introduced into consideration an orthorhombic unit cell, in which the axes a_1, a_2 are the diagonals of the West cell (Fig. 2 (b)). The Fraser lattice parameters a1, a2 in the paraphase are equal (a_1, a_2). In the ferrophase at a temperature of 116 K they are a_1 = 10.53 Å, a_2 = 10.44 Å, c = 6.90 Å.

Heat treatment in an electric field makes it possible to obtain a single-domain crystal [129].

As can be seen from fig. 2, the atoms of Potassium (K) and Phosphorus (P) are located at the nodes of the crystal lattice. Each of the phosphorus atoms is surrounded by four oxygen (O_2) atoms. The PO_4 groups form almost regular tetrahedra, the centers of which are phosphorus (P) atoms. Each PO_4 group is connected to four similar adjacent groups by hydrogen bonds about 2.4 Å long. The hydrogen bond is directed perpendicular to the c axis and always links the “upper” Oxygen of one PO_4 group with the “lower” Oxygen of the neighboring group, as shown in Fig. 2 (a).

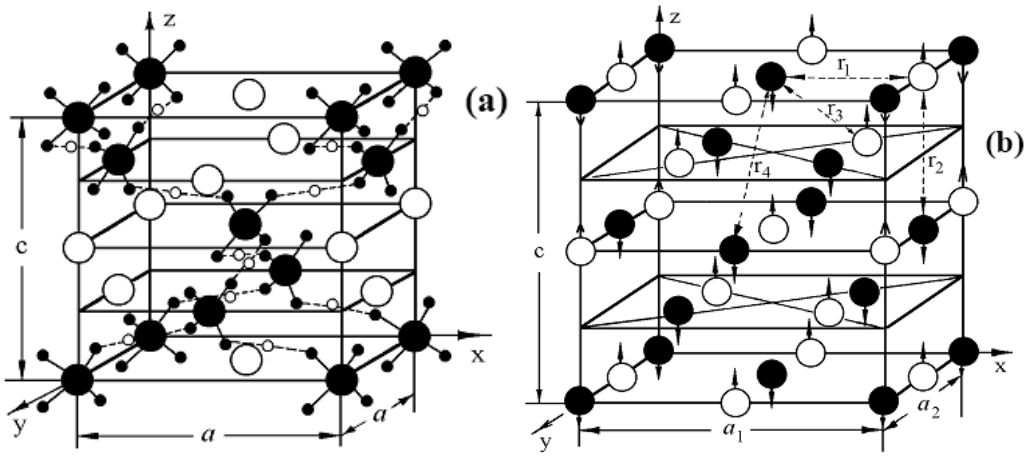

Fig. 2. Unit cell of potassium dihydrogen phosphate KH_2PO_4.
(a) Tetragonal structure of the paraelectric modification according to West [126].
(b) Orthorhombic structure of the Fraser ferroelectric modification (oxygen and hydrogen atoms not shown). Arrows indicate the directions of displacements of potassium (K) and phosphorus (P) atoms. The dotted straight lines mark the interstitial distances, the interaction between the K and P atoms at which are taken into account in the calculations.
○ – potassium atoms (K); ● – phosphorus atoms (P);
● – oxygen atoms (O); ○ – hydrogen atoms (H)

Each such bond has two equilibrium positions of hydrogen atoms at a distance of ~0.5 Å from each other, over which the latter are distributed statistically in the paraphase. In this case, there is no spontaneous polarization and deformation of the substance. With a decrease in temperature at T = –150°C = 123 K, the hydrogen atoms are ordered, which predominantly begin to be located in one of the above equilibrium positions [130-133], for example, near the "upper" or "lower" oxygen atoms, and a phase transition occurs into ferrophase. In this state, there are always only two hydrogen atoms near each PO_4 group. Potassium K atoms are surrounded by eight Oxygen atoms of different PO_4 tetrahedral groups, of which four (in the plane perpendicular to the c axis) are closer and four (two above and two below) are farther to the Potassium atoms. The ordering of hydrogen atoms changes the structure of the crystal: the lattice becomes rhombic, in which the square base of the West lattice lengthens along one of the diagonals and contracts along the other. The ordering of hydrogen atoms causes a significant shift of potassium (K) and phosphorus (P) atoms in opposite directions along the c axis (Fig. 2 (b)) relative to the oxygen frame, which practically does not shift. The displacement of potassium and phosphorus atoms causes spontaneous polarization and deformation of the crystal, which are directed along the c axis. In this case, the displacements of hydrogen atoms are perpendicular to the *c* axis and do not contribute to spontaneous polarization. When the sign of spontaneous polarization changes, hydrogen atoms shift from one equilibrium position to another [132].

When developing a statistical theory of spontaneous polarization of KDP crystals, we will consider the Fraser lattice and take into account the interaction of pairs of atoms KK, PP, KP (by P we mean the Phosphorus atom with its nearest four Hydrogen atoms) at distances marked by dashed straight lines with arrows in Fig. 2(b). Interactions of other atoms do not contribute to spontaneous polarization and deformation, so they can be ignored.

$$r_1' = \mathrm{a}_1 / 2, \quad r_1'' = \mathrm{a}_2 / 2, \quad r_2 = c / 2, \quad r_3 = \frac{1}{4}\sqrt{\mathrm{a}_1^2 + \mathrm{a}_2^2 + c^2},$$
$$r_4' = \frac{1}{2}\sqrt{\mathrm{a}_1^2 + c^2}, \quad r_4'' = \frac{1}{2}\sqrt{\mathrm{a}_2^2 + c^2}, \tag{1}$$

In the paraphase $a_1=a_2=a$, and the distances (1) are respectively equal to

$$r_1^o = r_1' = r_1'' = \mathrm{a}/2\ , \quad r_2^o = c/2\ , \quad r_3^o = \frac{1}{4}\sqrt{2\mathrm{a}^2 + c^2}\ , \qquad r_4^o = r_4' = r_4'' = \frac{1}{2}\sqrt{\mathrm{a}^2 + c^2}\ . \tag{2}$$

For potassium hydrogen phosphate, their numerical values in Å are as follows:

$$r_1' = 5{,}22\ ;\ r_1'' = 5{,}265\ ;\ r_2 = 3{,}45\ ;\ r_3 = 4{,}1\ ;\ r_4' = 6{,}26\ ;\ r_4'' = 6{,}29\ . \tag{3}$$

Since the distances r_1', r_1'' and r_4', r_4'' differ from each other insignificantly (by the second decimal place), we will take $r_1' = r_1''$ and $r_4' = r_4''$ in the calculations.

When the potassium and phosphorus atoms are ordered and displaced, the distances (1) change (decrease or increase) in comparison with their values (2) in the disordered state. Approximately one can put

$$r_1 \approx r_1' \approx r_1'' = r_1^o \pm \Delta_1\ , \quad r_2 = r_2^o \pm \Delta_2\ , \quad r_3 = r_3^o \pm \Delta_3\ , \qquad r_4 \approx r_4' \approx r_4'' = r_4^o \pm \Delta_4\ , \tag{4}$$

where the values Δ_i (i = 1, 2, 3, 4) are taken with the "+" or "–" sign, depending on the increase or decrease in the interatomic distance. When the potassium and phosphorus atoms are displaced, some interatomic distances (in planes perpendicular to the c axis) remain unchanged.

The crystal lattice of a KPD crystal can be conveniently divided into two sublattices for potassium atoms K and phosphorus P, respectively, which shift in opposite directions in the ferrophase. When ordering, potassium atoms shift upwards (Fig. 2(b)), let's call these shifts right *r*, and Phosphorus atoms - downwards. We will call them left *l*. In a disordered state and at the first stages of ordering, the displacements of the K and P atoms can be both right and left. The displacements of potassium and phosphorus atoms will be considered collinear. We denote the probabilities of right and left displacements of K and P atoms in sublattices

$$P_r^{(1)} = \frac{N_r^{(1)}}{N_1}\ , \quad P_1^{(1)} = \frac{N_1^{(1)}}{N_1}\ , \quad P_r^{(2)} = \frac{N_r^{(2)}}{N_2}\ , \quad P_1^{(2)} = \frac{N_1^{(2)}}{N_2}\ , \tag{5}$$

where $N=N_1=N_2$ are the numbers of sites (K and P atoms) in the sublattices, while the number of all lattice sites is equal to $2N$; $N_r^{(1)}$, $N_1^{(1)}$, $N_r^{(2)}$, $N_1^{(2)}$ - the number of K and P atoms, respectively, in the sublattices of the first and second with right *r* and left *l* shifts.

Probabilities (5) are related by relations

$$P_r^{(1)} + P_1^{(1)} = 1\ , \quad P_r^{(2)} + P_1^{(2)} = 1\ . \tag{6}$$

We introduce into consideration the order parameters for each of the sublattices

$$\xi_1 = P_r^{(1)} - P_1^{(1)}, \quad \xi_2 = P_r^{(2)} - P_1^{(2)}. \tag{7}$$

With complete disorder, when the probabilities of right and left displacements of all K and P atoms are the same, the order parameters are equal to zero $\xi_1 = \xi_2 = 0$. In full order, all Potassium atoms are right-handed $P_r^{(1)} = 1$, $P_1^{(1)} = 0$, and all Phosphorus atoms are left-handed $P_r^{(2)} = 0$, $P_1^{(2)} = 1$. In this case, the order parameters are maximum, equal to unity in absolute value $|\xi_1| = |\xi_2| = 1$ and opposite in sign $\xi_1 = -\xi_2$. The reversal of the signs of the order parameters

means that the roles of the first and second sublattices have been reversed. Thus, we have possible changes in the order parameters within

$$-1 \le \xi_1 \le +1 \quad , \qquad +1 \ge \xi_2 \ge -1 \, . \tag{8}$$

Equations (5), (6) allow us to express the probabilities $P_r^{(1)}$, $P_1^{(1)}$, $P_r^{(2)}$, $P_1^{(2)}$, in terms of the order parameters,

$$P_r^{(1)} = \frac{1+\xi_1}{2} \ , \ P_1^{(1)} = \frac{1-\xi_1}{2} \ , \ P_r^{(2)} = \frac{1+\xi_2}{2} \ , \ P_1^{(2)} = \frac{1-\xi_2}{2} \ . \tag{9}$$

Free and internal configurational energy. Equations of thermodynamic equilibrium taking into account the curie temperature

To solve the problems posed, it is necessary to calculate and study the free energy and thermodynamic potential of the crystal [134].

The free energy of the system is determined by the formula

$$F = U - kT \ln G \ , \tag{10}$$

where U is the internal configuration energy, G is the thermodynamic probability, k is the Boltzmann constant, and T is the absolute temperature.

The internal configuration energy is determined by the sum of the energies of the pair interaction of atoms KP, KK, PP at distances (1). Taking into account the interaction of all pairs of potassium and phosphorus atoms at distances taken in (2) and (4), the internal energy can be written as

$$\begin{aligned} U = & -N_{KP}^{(12)}(r_1)\upsilon_{KP}(r_1) - N_{KP}^{(12)}(r_1-\Delta_1)\upsilon_{KP}(r_1-\Delta_1) - \\ & -N_{KP}^{(12)}(r_2)\upsilon_{KP}(r_2) - N_{KP}^{(12)}(r_2-\Delta_2)\upsilon_{KP}(r_2-\Delta_2) - N_{KP}^{(12)}(r_2+\Delta_2)\upsilon_{KP}(r_2+\Delta_2) - \\ & -N_{KK}^{(11)}(r_3)\upsilon_{KK}(r_3) - N_{KK}^{(11)}(r_3-\Delta_3)\upsilon_{KK}(r_3-\Delta_3) - N_{KK}^{(11)}(r_3+\Delta_3)\upsilon_{KK}(r_3+\Delta_3) - \\ & -N_{PP}^{(22)}(r_3)\upsilon_{PP}(r_3) - N_{PP}^{(22)}(r_3-\Delta_3)\upsilon_{PP}(r_3-\Delta_3) - N_{PP}^{(22)}(r_3+\Delta_3)\upsilon_{PP}(r_3+\Delta_3) - \\ & -N_{KP}^{(12)}(r_3)\upsilon_{KP}(r_3) - N_{KP}^{(12)}(r_3-\Delta_3)\upsilon_{KP}(r_3-\Delta_3) - N_{KP}^{(12)}(r_3+\Delta_3)\upsilon_{KP}(r_3+\Delta_3) - \\ & -N_{KK}^{(11)}(r_4)\upsilon_{KK}(r_4) - N_{KK}^{(11)}(r_4-\Delta_4)\upsilon_{KK}(r_4-\Delta_4) - N_{KK}^{(11)}(r_4+\Delta_4)\upsilon_{KK}(r_4+\Delta_4) - \\ & -N_{PP}^{(22)}(r_4)\upsilon_{PP}(r_4) - N_{PP}^{(22)}(r_4-\Delta_4)\upsilon_{PP}(r_4-\Delta_4) - N_{PP}^{(22)}(r_4+\Delta_4)\upsilon_{PP}(r_4+\Delta_4) \, , \end{aligned} \tag{11}$$

Where $N_{\alpha\beta}^{(ij)}(r_n)$, $N_{\alpha\beta}^{(ij)}(r_n \pm \Delta_n)$ are the numbers of pairs of atoms of the type α, β = K, P, located at sites of type i, j = 1, 2, which are located at distances r_n or $r_n \pm \Delta_n$ (n = 1, 2, 3, 4), indicated in brackets, and the quantities are the energies $\upsilon_{\alpha\beta}(r_n)$, $\upsilon_{\alpha\beta}(r_n \pm \Delta_n)$, taken with the opposite sign, of the interaction of pairs of atoms α, β = K, P respectively, at distances r_n and $r_n \pm \Delta_n$. In formula (11), the superscripts "o" of the quantities r_n are omitted.

Below, the energy of interatomic interaction will be written in the form

$$\begin{aligned} & \upsilon_{KP}(r_1) = \upsilon_{KP}^{(1)} \ , \quad \upsilon_{KP}(r_1+\Delta_1) = \upsilon_{KP}^{(1)} \pm \delta_{KP}^{(1)} \ , \\ & \upsilon_{KP}(r_2) = \upsilon_{KP}^{(2)} \ , \quad \upsilon_{KP}(r_2 \pm \Delta_2) = \upsilon_{KP}^{(2)} \pm \delta_{KP}^{(2)} \ , \\ & \upsilon_{KK}(r_3) = \upsilon_{KK}^{(3)} \ , \quad \upsilon_{KK}(r_3 \pm \Delta_3) = \upsilon_{KK}^{(3)} \pm \delta_{KK}^{(3)} \ , \\ & \upsilon_{PP}(r_3) = \upsilon_{PP}^{(3)} \ , \quad \upsilon_{PP}(r_3 \pm \Delta_3) = \upsilon_{PP}^{(3)} \pm \delta_{PP}^{(3)} \ , \\ & \upsilon_{KP}(r_3) = \upsilon_{KP}^{(3)} \ , \quad \upsilon_{KP}(r_3 \pm \Delta_3) = \upsilon_{KP}^{(3)} \pm \delta_{KP}^{(3)} \ , \\ & \upsilon_{KK}(r_4) = \upsilon_{KK}^{(4)} \ , \quad \upsilon_{KK}(r_4 \pm \Delta_4) = \upsilon_{KK}^{(4)} \pm \delta_{KK}^{(4)} \ , \\ & \upsilon_{PP}(r_4) = \upsilon_{PP}^{(4)} \ , \quad \upsilon_{PP}(r_4 \pm \Delta_4) = \upsilon_{PP}^{(4)} \pm \delta_{PP}^{(4)} \ . \end{aligned} \tag{12}$$

The calculation of the number of pairs $N_{\alpha\beta}^{(ij)}(r_n)$, $N_{\alpha\beta}^{(ij)}(r_n \pm \Delta_n)$ for the structure under study in Fig. 2 (b) gives the following expressions

$$
\begin{aligned}
&\mathrm{N}_{\mathrm{KP}}^{(12)}(\mathrm{r}_1) = 4\mathrm{N}(\mathrm{P}_{\mathrm{r}}^{(1)}\mathrm{P}_{\mathrm{r}}^{(2)} + \mathrm{P}_{\mathrm{l}}^{(1)}\mathrm{P}_{\mathrm{l}}^{(2)}) = 0\,,\\
&\mathrm{N}_{\mathrm{KP}}^{(12)}(\mathrm{r}_2) = 2\mathrm{N}(\mathrm{P}_{\mathrm{r}}^{(1)}\mathrm{P}_{\mathrm{r}}^{(2)} + \mathrm{P}_{\mathrm{l}}^{(1)}\mathrm{P}_{\mathrm{l}}^{(2)}) = 0\,,\\
&\mathrm{N}_{\mathrm{KK}}^{(11)}(\mathrm{r}_3) = 2\mathrm{N}(\mathrm{P}_{\mathrm{r}}^{(1)^2} + \mathrm{P}_{\mathrm{l}}^{(1)^2}) = 2\mathrm{N}\,,\\
&\mathrm{N}_{\mathrm{PP}}^{(22)}(\mathrm{r}_3) = 2\mathrm{N}(\mathrm{P}_{\mathrm{r}}^{(2)^2} + \mathrm{P}_{\mathrm{l}}^{(2)^2}) = 2\mathrm{N}\,,\\
&\mathrm{N}_{\mathrm{KP}}^{(12)}(\mathrm{r}_3) = 4\mathrm{N}(\mathrm{P}_{\mathrm{r}}^{(1)}\mathrm{P}_{\mathrm{r}}^{(2)} + \mathrm{P}_{\mathrm{l}}^{(1)}\mathrm{P}_{\mathrm{l}}^{(2)}) = 0\,,\\
&\mathrm{N}_{\mathrm{KK}}^{(11)}(\mathrm{r}_4) = 4\mathrm{N}(\mathrm{P}_{\mathrm{r}}^{(1)^2} + \mathrm{P}_{\mathrm{l}}^{(1)^2}) = 4\mathrm{N}\,,\\
&\mathrm{N}_{\mathrm{PP}}^{(22)}(\mathrm{r}_4) = 4\mathrm{N}(\mathrm{P}_{\mathrm{r}}^{(2)^2} + \mathrm{P}_{\mathrm{l}}^{(2)^2}) = 4\mathrm{N}\,,\\
&\mathrm{N}_{\mathrm{KP}}^{(12)}(\mathrm{r}_1 + \Delta_1) = 4\mathrm{N}(\mathrm{P}_{\mathrm{r}}^{(1)}\mathrm{P}_{\mathrm{l}}^{(2)} + \mathrm{P}_{\mathrm{r}}^{(2)}\mathrm{P}_{\mathrm{l}}^{(1)}) = 4\mathrm{N}\,,\\
&\mathrm{N}_{\mathrm{KP}}^{(12)}(\mathrm{r}_2 \pm \Delta_2) = \mathrm{N}(\mathrm{P}_{\mathrm{r}}^{(1)}\mathrm{P}_{\mathrm{l}}^{(2)} + \mathrm{P}_{\mathrm{r}}^{(2)}\mathrm{P}_{\mathrm{l}}^{(1)}) = \mathrm{N}\,,\\
&\mathrm{N}_{\mathrm{KK}}^{(11)}(\mathrm{r}_3 \pm \Delta_3) = 2\mathrm{N}\mathrm{P}_{\mathrm{r}}^{(1)}\mathrm{P}_{\mathrm{l}}^{(1)} = 0\,,\\
&\mathrm{N}_{\mathrm{PP}}^{(22)}(\mathrm{r}_3 \pm \Delta_3) = 2\mathrm{N}\mathrm{P}_{\mathrm{r}}^{(2)}\mathrm{P}_{\mathrm{l}}^{(2)} = 0\,,\\
&\mathrm{N}_{\mathrm{KP}}^{(12)}(\mathrm{r}_3 \pm \Delta_3) = 2\mathrm{N}(\mathrm{P}_{\mathrm{r}}^{(1)}\mathrm{P}_{\mathrm{l}}^{(2)} + \mathrm{P}_{\mathrm{r}}^{(2)}\mathrm{P}_{\mathrm{l}}^{(1)}) = 2\mathrm{N}\,,\\
&\mathrm{N}_{\mathrm{KK}}^{(11)}(\mathrm{r}_4 \pm \Delta_4) = 4\mathrm{N}\mathrm{P}_{\mathrm{r}}^{(1)}\mathrm{P}_{\mathrm{l}}^{(1)} = 0\,,\\
&\mathrm{N}_{\mathrm{PP}}^{(22)}(\mathrm{r}_4 \pm \Delta_4) = 4\mathrm{N}\mathrm{P}_{\mathrm{r}}^{(2)}\mathrm{P}_{\mathrm{l}}^{(2)} = 0.
\end{aligned}
\tag{13}
$$

On the right in formulas (13), the values of the numbers of the pairs under consideration are written out with complete ordering, when $P_r^{(1)} = 1$, $P_{\mathrm{l}}^{(1)} = 0$, $P_r^{(2)} = 1$, $P_{\mathrm{l}}^{(2)} = 1$.

Substituting the numbers of atomic pairs (13) into formula (11) for the energy U, taking into account relations (6), we find the internal energy of the crystal, expressed in terms of probabilities (5), in the form

$$
\begin{aligned}
U = -2N\Big[&2\upsilon_{KP}^{(1)} + \upsilon_{KP}^{(2)} + \left(\upsilon_{KK}^{(3)} + \upsilon_{PP}^{(3)} + 2\upsilon_{KP}^{(3)}\right) + 2\left(\upsilon_{KK}^{(4)} + \upsilon_{PP}^{(4)}\right) + \\
&+ 2\left(P_r^{(1)}P_{\mathrm{l}}^{(2)} + P_r^{(2)}P_{\mathrm{l}}^{(1)}\right)\delta\Big]\,, \quad \delta = \delta_{KP}^{(1)}\,.
\end{aligned}
\tag{14}
$$

Substituting probabilities (9) into the resulting formula (14), we find the configuration energy

$$
U = -2N\left(\upsilon - \xi_1\xi_2\delta\right)\,, \tag{15}
$$

as a function of order parameters ξ_1, ξ_2 and energy constants υ and δ. In (15), the following notation is introduced:

$$
\upsilon = 2\upsilon_{KP}^{(1)} + \upsilon_{KP}^{(2)} + \left(\upsilon_{KK}^{(3)} + \upsilon_{PP}^{(3)} + 2\upsilon_{KP}^{(3)}\right) + 2\left(\upsilon_{KK}^{(4)} + \upsilon_{PP}^{(4)}\right) - \delta\,. \tag{16}
$$

The thermodynamic probability G is determined by the rules of combinatorics

$$
G = \frac{N_1!}{N_r^{(1)}!N_{\mathrm{l}}^{(1)}!} \cdot \frac{N_2!}{N_r^{(2)}!N_{\mathrm{l}}^{(2)}!}\,. \tag{17}
$$

Taking into account the Stirling formula lnX! = X(lnX – 1), which is valid for large numbers X, taking into account formulas (5) for the probabilities $P_r^{(1)}$, $P_{\mathrm{l}}^{(1)}$, $P_r^{(2)}$, $P_{\mathrm{l}}^{(2)}$, we find the natural logarithm of the thermodynamic probability G in the form

$$\ln G = -N\left(P_r^{(1)} \ln P_r^{(1)} + P_1^{(1)} \ln P_1^{(1)} + P_r^{(2)} \ln P_r^{(2)} + P_1^{(2)} \ln P_1^{(2)}\right), \tag{18}$$

which, taking into account formulas (9), takes the form

$$\begin{aligned} \ln G = -\frac{1}{2} N[&\left(1+\xi_1\right)\ln\frac{1+\xi_1}{2} + \left(1-\xi_1\right)\ln\frac{1-\xi_1}{2} \\ &+\left(1+\xi_2\right)\ln\frac{1+\xi_2}{2} + \left(1-\xi_2\right)\ln\frac{1-\xi_2}{2}]. \end{aligned} \tag{19}$$

Substituting relations (14), (18) or (15), (19) for the quantities U and G into formula (10) for the free energy F, we find the free energy of the crystal, expressed in terms of probabilities $P_r^{(1)}$, $P_1^{(1)}$, $P_r^{(2)}$, $P_1^{(2)}$ or in terms of order parameters ξ_1, ξ_2, respectively, in the form

$$\begin{aligned} F = &-2N\left[\upsilon - \delta + 2\left(P_r^{(1)} P_1^{(2)} + P_r^{(2)} P_1^{(1)}\right)\delta\right] + \\ &+kTN\left[P_r^{(1)} \ln P_r^{(1)} + P_1^{(1)} \ln P_1^{(1)} + P_r^{(2)} \ln P_r^{(2)} + P_1^{(2)} \ln P_1^{(2)}\right] \end{aligned} \tag{20}$$

or

$$\begin{aligned} F = &-2N\left(\upsilon - \xi_1\xi_2\delta\right) + \frac{1}{2} kTN[\left(1+\xi_1\right)\ln\frac{1+\xi_1}{2} + \\ &+\left(1-\xi_1\right)\ln\frac{1-\xi_1}{2} + \left(1+\xi_2\right)\ln\frac{1+\xi_2}{2} + \left(1-\xi_2\right)\ln\frac{1-\xi_2}{2}]. \end{aligned} \tag{21}$$

The last formula determines the dependence of the free energy of the crystal on temperature T, order parameters ξ_1, ξ_2 and energy constants υ, δ.

The change in the free energy of the system when the order parameters change from values ξ_1, ξ_2 to zero per one site of the crystal lattice is equal to

$$\begin{aligned} f = \frac{F\left(\xi_1,\ \xi_2\right) - F(O)}{2N} = &-\upsilon + \xi_1\xi_2\delta + \frac{1}{4} kT[\left(1+\xi_1\right)\ln\frac{1+\xi_1}{2} + \\ &+\left(1-\xi_1\right)\ln\frac{1-\xi_1}{2} + \left(1+\xi_2\right)\ln\frac{1+\xi_2}{2} + \left(1-\xi_2\right)\ln\frac{1-\xi_2}{2} + 2\ln 2]. \end{aligned} \tag{22}$$

The conditions for thermodynamic equilibrium of the system are determined by the equalities

$$\partial f / \partial \xi_1 = 0, \quad \partial f / \partial \xi_2 = 0, \tag{23}$$

which, taking into account formula (22), give the relations

$$kT \ln\frac{1+\xi_1}{1-\xi_1} = -4\delta\xi_2, \quad kT \ln\frac{1+\xi_2}{1-\xi_2} = -4\delta\xi_1. \tag{24}$$

The resulting equations (24) admit solutions: $\xi_2 = -\xi_1$ and $\xi_2 = \xi_1$. With such replacements, the first equation in (24) transforms into the second and vice versa. We are interested in the first solution

$$\xi = \xi_1 = -\xi_2, \tag{25}$$

which corresponds to displacements of potassium and phosphorus atoms in opposite directions. In this case, two equations of thermodynamic equilibrium (24) of the system turn into one.

Free energy (22) and equilibrium state equations (24) take the form

$$f = -\upsilon - \xi^2\delta + \frac{1}{2}kT\left[(1+\xi)\ln\frac{1+\xi}{2} + (1-\xi)\ln\frac{1-\xi}{2} + 2\ln 2\right], \tag{26}$$

$$kT\ln\frac{1+\xi}{1-\xi} = 4\delta\xi\ . \tag{27}$$

Assuming in equation (27) $\xi\to 0$, we find the phase transition temperature (Curie point)

$$kT_o = 2\delta = \omega_o \tag{28}$$

The quantity ω_o is the energy of ordering the system.

In the process of ordering, the value of ω may depend on interatomic distances, taking into account the latter, on the order parameter ξ. Calculations show [134] that the ordering energy in the general case is a fractional rational function with polynomials in the numerator and denominator of the fourth degree in the order parameter ξ. In special cases, this dependence is simplified, and the value ω may turn out to be a quadratic function of the parameter ξ. Consider the last case when

$$\omega = \omega_o + \alpha\xi^2\ . \tag{29}$$

In this case, the temperature dependence of the order parameter $\xi = \xi(T)$ is determined by the formula

$$kT\ln\frac{1+\xi}{1-\xi} = 2\left(\omega_o + \alpha\xi^2\right)\xi, \tag{30}$$

with ordering temperature (28).

On fig. Figure 3 shows graphs of the temperature dependence of the order parameter, constructed by formula (30) for various values of the dimensionless energy parameter α/ω_o. Experimentally, this dependence is characterized by graphs of the temperature dependence of the degree of spontaneous polarization P(T) fig. 1(a).

As can be seen from fig. 3, the nature of the dependence ξ(T)near the Curie point strongly depends on the value of the energy parameter α/ω_o. For negative values of α, the graphs ξ(T) near T_0 turn out to be gentle. If $\alpha>0$, the graphs in the considered temperature range (T_0) become steep, and with an increase in the numerical value of α, the phase transition can even turn out to be a first-order transformation.

From a comparison of the calculated graphs in Fig. 3 with the experimental ones in Figs. 2 (a), we can conclude that in KDP crystals, in which the transformation of the paraphase into the ferrophase occurs according to the type of second-order transition, close to the first, the dependence $\xi = \xi$(T) should be described by function (30) with a positive value of the energy parameter α, for example, α/ω_o=0,2. In this case, the order parameter, like the spontaneous polarization, changes continuously but abruptly near the Curie temperature.

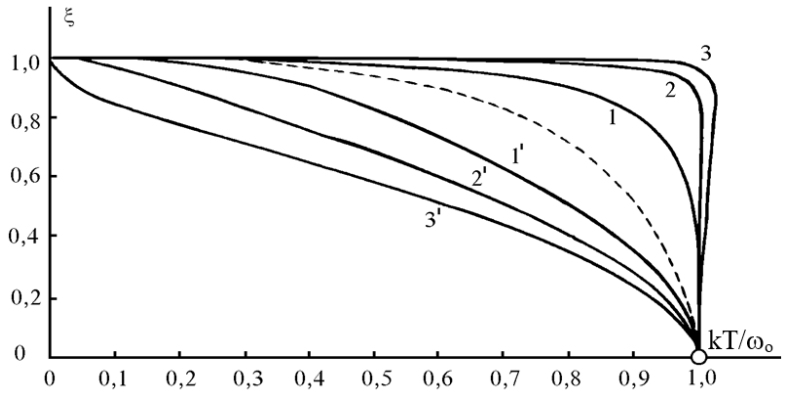

Fig. 3. Calculated graphs of the temperature dependence of the order parameter of spontaneous polarization, built according to formula (30) for the values of the energy parameter $\alpha/\omega_o=0$ (dashed curve), ± 0,2; ± 0,4; ± 0,6 (curves 1, 2, 3 for the "+" sign and 1′, 2′, 3′ for the "–" sign)

Configuration heat capacity

Knowing the internal energy of the system, which, per one lattice site at $\xi = \xi_1 = -\xi_2$, taking into account formulas (15) and (29), is equal to

$$u = \frac{U}{2N} = -\frac{1}{2}\left(\omega_o + \alpha\xi^2\right)\xi^2, \tag{31}$$

formula it is possible to estimate the temperature dependence of the heat capacity by the formula

$$C = \frac{\partial u}{\partial T} = \frac{\partial u}{\partial \xi}\frac{d\xi}{dT} = -\left(\omega_o + 2\alpha\xi^2\right)\xi\frac{d\xi}{dT} . \tag{32}$$

In this case, the temperature dependences of the values of ξ and $\frac{d\xi}{dT}$ must be determined from formula (30). Differentiating equality (30) with respect to temperature, we find the derivative $d\xi / dT$

$$\frac{d\xi}{dT} = k\ln\frac{1+\xi}{1-\xi}\Bigg/ 2\left(\omega_o + 6\alpha\xi^2 - \frac{kT}{1-\xi^2}\right), \tag{33}$$

and then the heat capacity C in units of the Boltzmann constant in the form

$$\frac{C}{k} = \frac{\left(1+2\frac{\alpha}{\omega_o}\xi^2\right)\xi\ln\frac{1+\xi}{1-\xi}}{2\left(\frac{kT/\omega_o}{1-\xi^2} - 1 - 6\frac{\alpha}{\omega_o}\xi^2\right)} . \tag{34}$$

On fig. Figure 4 shows graphs of the C(T) function in the phase transition region, plotted according to formula (34) for various values of the dimensionless energy parameter α/ω_o. In this case, for each value of α/ω_o and a certain temperature, the value of the order parameter ξ was determined by formula (30), which was then substituted into formula (34).

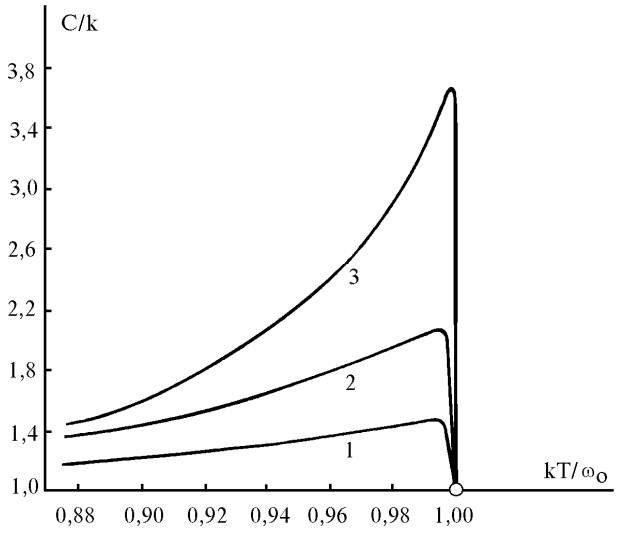

Fig. 4. Calculated graphs of the temperature dependence of the configurational heat capacity of the crystal in the phase transition region, constructed according to the formula (34) taking into account the dependence ξ(T) (30) for the values of the energy parameter α/ω_o=0; 0,05; 0,1 (curves 1, 2, 3)

As can be seen from fig. 4, at the phase transition point, the configuration heat capacity increases and has a peak, which is the sharper and higher, the greater the value of α/ω_o. This means that in KDP crystals, the paraelectric-ferroelectric phase transition occurs at positive values of α/ω_o and should be close to a first-order transition. At the same time, with an increase in the coefficient α/ω_o, the heat capacity jump at the Curie point (T_0) increases.

Comparison of the calculated graph in Fig. 4 with the experimental graphs in Fig. 1 (c) and (d) indicates a qualitative agreement between theory and experiment.

Thermodynamic potential. Dependence of the order parameter on the electric field strength

If the crystal under study is in an external electric field with a strength $\bar{E}$ and under the action of an external mechanical oriented voltage $\bar{\sigma}$, then its state will be determined by the thermodynamic potential. In this case, the degree of spontaneous polarization P and deformation X will be proportional to the order parameter ξ:

$$P = \mathrm{k}\xi\ , \qquad X = \mathrm{k}'\xi\ . \tag{35}$$

Therefore, the thermodynamic potential can be determined by the formula

$$\Phi = F \pm \bar{E}\ \bar{P} \pm \bar{\sigma}\ \bar{X} = F \pm 2N\mathrm{k}E\xi - 2N\mathrm{k}'\sigma\xi\ , \tag{36}$$

where the signs "+" and "–" correspond to the work of external forces or the work done by the system.

Taking into account formulas (26), (35) and (36), the change in the thermodynamic potential per one site of the crystal lattice will be equal to

$$\phi = \frac{\Phi(\xi) - \Phi(O)}{2N} = -\frac{1}{2}\left(\omega_o + \alpha\xi^2\right)\xi^2 + \\ + \frac{1}{2}kT\left[(1+\xi)\ln\frac{1+\xi}{2} + (1-\xi)\ln\frac{1-\xi}{2} + 2\ln 2\right] - \mathrm{k}E\xi - \mathrm{k}'\sigma\xi\ . \tag{37}$$

The equilibrium state equation takes the form

$$-\left(\omega_o + 2\alpha\xi^2\right)\xi + \frac{1}{2}kT\ln\frac{1+\xi}{1-\xi} - \mathrm{k}E - \mathrm{k}'\sigma = 0\ . \tag{38}$$

In the absence of external forces (E=σ=0), assuming in (38) $\xi \to 0$ and taking into account that $\omega_o = kT_o$, we find the temperature dependence of the order parameter near the Curie point in the form

$$\xi = \sqrt{\frac{k(T - T_o)}{2\alpha}} \ . \tag{39}$$

It follows from this relation that in the absence of order at temperature $T>T_0$ we have $\alpha>0$. If $T<T_0$, then at the phase transition of the second kind should be $\alpha<0$. However, during phase transitions close to the first order, the phase transformation temperature may somewhat exceed the Curie temperature, and, as was found out above, it is possible that in an ordered state near the Curie point we will have $T>T_0$ and $\alpha>0$.

Assuming in equation (38) σ=0, we find the relation

$$\mathrm{k}E = \left(2\alpha\xi^2 + \omega_o\right)\xi - \frac{1}{2}kT\ln\frac{1+\xi}{1-\xi} \ , \tag{40}$$

which determines the dependence of the order parameter on the strength of the external field ξ=ξ(E). By setting in equation (40) all possible numerical values of the order parameter $0 \le |\xi| \le 1$, it is possible to determine the value of kE for certain temperatures and plot graphs ξ(E) for the given temperatures.

It is convenient to introduce into consideration the dimensionless quantity

$$x = (T - T_o) / T_o \tag{41}$$

and establish dependence ξ(E) for different values of x. In this case, formula (40) takes the form

$$\frac{\mathrm{k}}{\omega_o}E = \left(2\frac{\alpha}{\omega_o}\xi^2 + 1\right)\xi - \frac{1}{2}(1-x)\ln\frac{1+\xi}{1-\xi} \ . \tag{42}$$

Near the Curie point at $\xi \to 0$, taking into account that $\ln\frac{1+\xi}{1-\xi} \approx 2\xi$, instead of formula (42), one can obtain an approximate formula

$$\frac{\mathrm{k}}{\omega_o}E = 2\frac{\alpha}{\omega_o}\xi^3 + x\xi \ . \tag{43}$$

From formulas (42), (43) it follows that the dependence ξ(E) must be non-linear.

On fig. Figure 5 shows the graphs of the dependence ξ = ξ(E), constructed according to the approximate formula (43) (solid curves) and the more accurate formula (42) (dashed curves) for different values of x and the energy parameter α/ω_o = 0.5. As can be seen from fig. 5, the dependence ξ(E) is non-linear, but with an increase in the value of x, it approaches linear. Graphs corresponding to the value x=1, built according to formulas (42), (43), coincide. For x<1, the dotted curves corresponding to the more precise formula (42) pass above, and for x>1, they pass below the continuous curves constructed using the approximate formula (43). In addition, dotted curve 2 has a feature in the form of the presence of an extremum of the value E. This can be explained by the fact that positive values of the parameter $\alpha>0$ correspond to a first-order phase transition. Section AB of curve 2 (Fig. 5) corresponds to an unstable state and is not realized. At the value of the order parameter corresponding to point A ($\xi \approx 0.9$), a sharp decrease in the degree of crystal polarization to zero should occur during phase transitions of the first

kind. Therefore, the feature revealed in the calculations should not manifest itself experimentally.

Comparison of calculated graphs in Figs. 5 for $\alpha>0$ with experimental curves in fig. 1(b) indicate their qualitative correspondence.

Dielectric susceptibility

Formulas (42) or (43) make it possible to estimate the dielectric susceptibility χ or the permittivity $\varepsilon=1+\chi$ of a crystal.

The dielectric susceptibility is given by

$$\varepsilon_o \chi = \partial P / \partial E = \mathrm{k}\partial\xi / \partial E \ , \tag{44}$$

where ε_o is the electrical constant, which we include in the coefficient k.

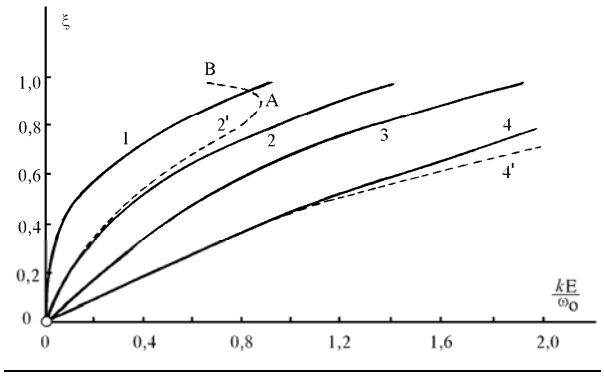

Fig. 5. Calculated graphs of the order parameter, which characterizes the degree of spontaneous polarization, for different temperatures ($x = (T - T_o)/T_o$) depending on the strength of the external electric field, constructed according to formulas (43) (continuous curves 1, 2, 3, 4) and (42) (dashed curves 2′, 4′) for $\alpha/\omega_o = 0.5$ and numerical values of x = 0; 0.5; 1; 2 (curves 1, 2, 3, 4)

For potassium dihydrogen phosphate, the permittivity is a tensor with components ε_{11}, ε_{22}, ε_{33}. We will consider the component along the polar axis *c* $\varepsilon_c = \varepsilon_{33}$ and the corresponding dielectric susceptibility χ.

Using the approximate formula (43), which is valid near the Curie point, we find the relation

$$\mathrm{k}^2 \frac{1}{\chi} = 6\alpha\xi^2 + x \ , \tag{45}$$

which, taking into account formulas (39) and (41), gives

$$\mathrm{k}^2 \frac{1}{\chi} = \begin{cases} 2k(T - T_o) & at \quad \xi \neq 0 \ , \\ -k(T - T_o) & at \quad \xi = 0 \ . \end{cases} \tag{46}$$

As we can see, from the obtained expressions (46), in this case, the rule of negative two is fulfilled:

$$\left(\frac{\partial E}{\partial P}\right)_{\xi\neq 0} \Big/ \left(\frac{\partial E}{\partial P}\right)_{\xi=0} = -2 \ . \tag{47}$$

Using a more precise formula (42), we obtain the inverse dielectric susceptibility in the form:

$$\frac{k^2}{\omega_o}\frac{1}{\chi}=\begin{cases}-2x\left[1+\dfrac{1+x}{2\left(x-\dfrac{2\alpha}{\omega_o}\right)}\right] & \text{at} \quad \xi\neq 0\\ x \quad \text{at} \quad \xi=0\,.\end{cases} \tag{48}$$

As we can see from these relations, the dependence of the inverse dielectric susceptibility on temperature $\frac{1}{\chi}(x)$ in the absence of dipole ordering (ξ=0) is linear. However, at ($x\to 0$) this dependence is already nonlinear. However, near the Curie point (($x\to 0$), the dependence $\frac{1}{\chi}(x)$ is close to linear, and therefore the rule of negative two is valid. The dielectric susceptibility at $x\to 0$ ($T\to T_o$) increases to infinity ($\chi\to\infty$).

Comparison of the obtained calculated graphs with experimental fig. 1 (e) for the permittivity again indicates their qualitative correspondence. These patterns are illustrated by the graphs in Fig. 6, which are built for the energy parameter $2\alpha/\omega_o = -0{,}15$. The dependence $1/\varepsilon_c(T)$ for a KH_2PO_4 crystal at $T>T_o$ = 123 K is linear. At $T\to T_o$, the experimental graph $\varepsilon_c(T)$ has a sharp peak.

We also note that since the order parameters of spontaneous polarization and deformation coincide in the crystals under study, the temperature dependences for the direct and inverse elastic compliance can be obtained similar to those obtained for the direct and inverse dielectric susceptibility. To do this, in equation (38) one should take E=0, as a result, we obtain the dependence $\xi(\sigma)$, similar to that following from equation (40) for $\xi(E)$. Such studies make it possible to explain and justify the increase in spontaneous deformation X with decreasing temperature at $T\to T_o$ (Fig. 1(g)), a sharp decrease in the elastic constant c_{66} (Fig. 1 (h)) and the shear modulus G (Fig. 1 (i)) at the Curie point. In this case, in accordance with theoretical calculations, the G(T) dependence of the KH_2PO_4 crystal near the Curie temperature should be linear, which also manifests itself experimentally, and the slopes of the G(T) curve at $T < T_o$ and $T > T_o$ are such that the tangent of the slope of the first exceeds that in the case of $T > T_o$.in absolute value.

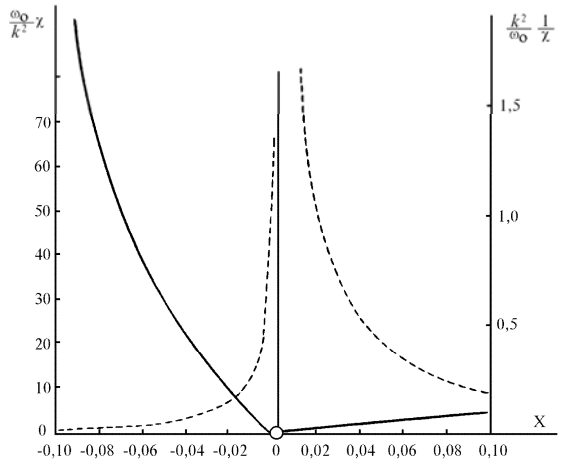

Fig. 6. Calculated graphs of the temperature dependence ($x = (T - T_o)/T_o$) of the inverse $1/\chi$ (continuous curves) and direct χ (dashed curves) of the dielectric susceptibility, constructed by formula (48) for the numerical value of the energy parameter $2\alpha/\omega_o = -0.15$

Conclusions

Thus, the developed statistical theory of spontaneous polarization and deformation in nanodispersed powders KDP crystals, taking into account the interpretation of the paraelectric-ferroelectric phase transition as a type of ordering, made it possible to establish and explain the

temperature dependence of the order parameter, the nature of this dependence, close to a first-order transition, the dependence of the order parameter on the strength of the external electric field, justify the manifestation of its nonlinearity, clarify the feature of the temperature dependence of the configurational heat capacity and show that it is close to the experimental one precisely for the case of a phase transition similar in kind to the first one, and also show that the temperature dependences of the direct and inverse susceptibility are such that the Curie-Weiss law is valid (nonlinear dependence of the value $1/\chi$ on temperature) and near the Curie point the rule of negative two is feasible.

All revealed regularities were compared with experimental data, a qualitative agreement between the results of the calculation analysis and experiment was obtained, which indicates the correctness (adequacy) of the developed statistical theory.

References

1. Zaginaichenko S.Y., Lysenko E.A., Golovchenko T.N., Javadov N.F. The forming peculiarities of C_{60} molecule. *NATO Science for Peace and Security Series C: Environmental Security*. 2008. **PartF2:** 53-65.
2. Zolotarenko Ol. D., Rudakova E. P., Akhanova N. Yu., Zolotarenko An. D., Shchur D. V., Matysina Z. A., Gabdullin M. T., Ualkhanova M., Gavrylyuk N. A., Zolotarenko A. D., Chymbai M. V., Zagorulko I. V. Comparative Analysis of Products of the Fullerenes' and Carbon-Nanostructures' Synthesis Using the SIGE and FGDG-7 Grades of Graphite. *Nanosistemi, nanomateriali, nanotehnologii.* 2022. **20**(3): 725.
3. Gun'ko V.M., Turov V.V., Zarko V.I., Prykhod'Ko G.P., Krupska T.V., Golovan A.P., Skubiszewska-Zięba J., Charmas B., Kartel M.T. Unusual interfacial phenomena at a surface of fullerite and carbon nanotubes. *Chemical Physics*. 2015. **459**: 172-185.
4. Nishchenko M.M., Likhtorovich S.P., Dubovoy A.G., Rashevskaya T.A. Positron annihilation in C_{60} fullerites and fullerene-like nanovoids. *Carbon.* 2003. **41**(7): 1381.
5. Lad'yanov V.I., Nikonov, R.M., Larionova N.S., Aksenova V.V., Mukhgalin V.V., Rud' A.D. Deformation-induced changes in the structure of fullerites $C_{60/70}$ during their mechanical activation. *Physics of the Solid State*. 2013. **55**(6): 1319.
6. Matysina Z.A., Zolotarenko Ol.D., Rudakova O.P., Akhanova N.Y., Pomytkin A.P., Zolotarenko An.D., Shchur D.V., Gabdullin M.T., Ualkhanova M., Gavrylyuk N.A., Zolotarenko A.D., Chymbai M.V., Zagorulko I.V. Iron in Endometallofullerenes. *Prog. Phys. Met.* 2022. **23**(3): 510.
7. Kartel M.T., Voitko K.V., Grebelna Y.V., Zhuravskyi S.V., Ivanenko K.O., Kulyk T.V., Makhno S.M., Sementsov Y.I. Changes in the structure and properties of graphene oxide surfaces during reduction and modification. *Himia, Fizika ta Tehnologia Poverhni*. 2022. **13**(2): 179.
8. Rud A.D., Kiryan I.M. Quantitative analysis of the local atomic structure in disordered carbon. *Journal of Non-Crystalline Solids*. 2014. **386**: 1.
9. Sementsov Yu.I., Cherniuk O.A., Zhuravskyi S.V., Bo W., Voitko K.V., Bakalinska O.M., Kartel, M.T. Synthesis and catalytic properties of nitrogen-containing carbon nanotubes. *Himia, Fizika ta Tehnologia Poverhni*. 2021. **12**(2): 135.
10. Barany S., Kartel' N., Meszaros R. Electrokinetic potential of multilayer carbon nanotubes in aqueous solutions of electrolytes and surfactants. *Colloid Journal*. 2014. **76**(5): 509.
11. Schur D.V., Dubovoy A.G., Zaginaichenko S.Yu., Adejev V.M., Kotko A.V., Bogolepov V.A., Savenko A.F., Zolotarenko A.D., Firstov S.A., Skorokhod V.V. Synthesis of carbon nanostructures in gaseous and liquid medium. *NATO Security through Science Series A: Chemistry and Biology*. 2007: 199.
12. Zaginaichenko S.Y., Matysina Z.A. The peculiarities of carbon interaction with catalysts during the synthesis of carbon nanomaterials. *Carbon.* 2003. **41**(7): 1349.

13. Boguslavskii L.Z., Rud' A.D., Kir'yan I.M., Nazarova N.S., Vinnichenko D.V. Properties of carbon nanomaterials produced from gaseous raw materials using high-frequency electrodischarge processing. *Surface Engineering and Applied Electrochemistry*. 2015. **51**(2): 105.
14. Matysina Z.A., Zolotarenko Ol.D., Ualkhanova M., Rudakova O.P., Akhanova N.Y., Zolotarenko An.D., Shchur D.V., Gabdullin M.T., Gavrylyuk N.A., Zolotarenko O.D., Chymbai M.V., Zagorulko I.V. Electric Arc Methods to Synthesize Carbon Nanostructures. *Prog. Phys. Met*. 2022. 23(3): 528.
15. Yakymchuk O.M., Perepelytsina O.M., Rud A.D., Kirian I.M., Sydorenko M.V. Impact of carbon nanomaterials on the formation of multicellular spheroids by tumor cells. *Physica Status Solidi (A) Applications and Materials Science*. 2014. **211**(12): 2778.
16. Kartel N.T., Gerasimenko N.V., Tsyba N.N., Nikolaichuk A.D., Kovtun G.A. Synthesis and study of carbon sorbent prepared from polyethylene terephthalate. *Russian Journal of Applied Chemistry*. 2001. **74**(10): 1765.
17. Zolotarenko Ol.D, Ualkhanova M.N., Rudakova E.P., Akhanova N.Y., Zolotarenko An.D., Shchur D.V., Gabdullin M.T., Gavrylyuk N.A., Zolotarenko A.D., Chymbai M.V., Zagorulko I.V., Havryliuk O.O. Advantages and disadvantages of electric arc methods for the synthesis of carbon nanostructures. *Himia, Fizika ta Tehnologia Poverhni*. 2022. **13**(2): 209. [in Ukrainian]
18. Oreshkin V.I., Chaikovskii S.A., Labetskaya N.A., Ivanov Y.F., Khishchenko K.V., Levashov P.R., Kuskova N.I., Rud' A.D. Phase transformations of carbon under extreme energy action. *Technical Physics*. 2012. **57**(2): 198.
19. Rud A.D., Lakhnik A.M., Mikhailova S.S., Karban O.V., Surnin D.V., Gilmutdinov F.Z. Structure of Mg-C nanocomposites produced by mechano-chemical synthesis. J*ournal of Alloys and Compounds*. 2011. **509**(SUPPL. 2): S592.
20. Ushakova L.M., Ivanenko K.I., Sigareva N.V., Terets M.I., Kartel M.T., Sementsov Yu.I. Influence of nanofiller on the structure and properties of macromolecular compounds. *Physics and Chemistry of Solid State*. 2022. **23**(2): 394.
21. Sementsov Y., Prikhod'ko G., Kartel M., Tsebrenko M., Aleksyeyeva T., Ulyanchychi N. Carbon nanotubes filled composite materials. *NATO Science for Peace and Security Series C: Environmental Security*. 2011. **2**: 183.
22. Harea E., Stoček R., Storozhuk L., Sementsov Y., Kartel N. Study of tribological properties of natural rubber containing carbon nanotubes and carbon black as hybrid fillers. *Applied Nanoscience*. 2019. **9**(5): 899.
23. Gun'ko V.M., Turov V.V., Protsak I., Krupska T.V., Pakhlov E.M., Zhang D. Interfacial phenomena in composites with nanostructured succinic acid bound to hydrophilic and hydrophobic nanosilicas. *Colloids and Interface Science Communications*. 2020. **35**:100251.
24. Zolotarenko O.D., Rudakova E.P., Zolotarenko A.D., Akhanova N.Y., Ualkhanova M.N., Shchur D.V., Gabdullin M.T., Gavrylyuk N.A., Myronenko T.V., Zolotarenko A.D., Chymbai M.V., Zagorulko I.V., Tarasenko Yu.O., Havryliuk O.O. Platinum-containing carbon nanostructures for the creation of electrically conductive ceramics using 3D printing of CJP technology. *Himia, Fizika ta Tehnologia Poverhni*. 2022. **13**(3): 259. [in Ukrainian]
25. Zolotarenko Ol.D., Rudakova E.P., Akhanova N.Y., Zolotarenko An.D., Shchur D.V., Gabdullin M.T., Ualkhanova M., Sultangazina M., Gavrylyuk N.A., Chymbai M.V., Zolotarenko A.D., Zagorulko I.V., Tarasenko Yu.O. Plasmochemical Synthesis of Platinum-Containing Carbon Nanostructures Suitable for CJP 3D-Printing. *Metallofiz. NoveishieTekhnol*. 2022. **44**(3): 343.

26. Zolotarenko Ol.D., Rudakova E.P., Akhanova N.Y., Zolotarenko An.D., Shchur D.V., Gabdullin M.T., Ualkhanova M., Gavrylyuk N.A., Chymbai M.V., Myronenko T.V., Zagorulko I.V., Zolotarenko A.D., Havryliuk O.O. Electrically conductive composites based on TiO_2 and carbon nanostructures manufactured using 3D printing of CJP technology. *Himia, Fizika ta Tehnologia Poverhni*. 2022. **13**(4): 415.
27. Zolotarenko Ol.D., Rudakova E.P., Akhanova N.Y., Zolotarenko An.D., Shchur D.V., Gabdullin M.T., Ualkhanova M., Gavrylyuk N.A., Chymbai M.V., Tarasenko Yu. O., Zagorulko I.V., Zolotarenko A.D. Electric Conductive Composites Based on Metal Oxides and Carbon Nanostructures. *Metallofiz. Noveishie Tekhnol*. 2021. **43**(10): 1417. [in Ukrainian]
28. Fawzeia K. Biomedical application of KDP nano crystals. In: *NCRTMSA* (April, 2023, Tripoli, Libya). P.4.
29. Sementsov Yu.I., Prikhod'Ko G.P., Melezhik A.V., Aleksyeyeva T.A., Kartel M.T. Physicochemical properties and biocompatibility of polymer/carbon nanotubes composites. *Nanomaterials and Supramolecular Structures: Physics, Chemistry, and Applications*. 2010: 347.
30. Gun'ko V.M., Lupascu, T., Krupska T.V., Golovan A.P., Pakhlov E.M., Turov V.V. Influence of tannin on aqueous layers at a surface of hydrophilic and hydrophobic nanosilicas. *Colloids and Surfaces A: Physicochemical and Engineering Aspects*. 2017. **531**: 9.
31. Khamitova K.K., Kayupov B.A., Yegemova S.S., Gabdullin M.T., Abdullin Kh.A., Ismailov D.V., Kerimbekov D.S. The use of fullerenes as a biologically active molecule. *International Journal of Nanotechnology*. 2019. **16**(1-3):100.
32. Gun'ko V.M., Turov V.V., Krupska T.V., Tsapko M.D. Interactions of human serum albumin with doxorubicin in different media. *Chemical Physics*. 2017. **483-484**: 26.
33. Gun'ko V.M., Turov V.V., Krupska T.V., Protsak I.S., Borysenko M.V., Pakhlov E.M. Polymethylsiloxane alone and in composition with nanosilica under various conditions. *Journal of Colloid and Interface Science*. 2019. **541**: 213-225.
34. Krupska T.V., Turova A.A., Un'Ko V.M., Turov V.V. Influence of highly dispersed materials on physiological activity of yeast cells. *Biopolymers and Cell*. 2009. **25**(4): 290.
35. Stavitskaya S.S., Mironyuk T.I., Kartel' N.T., Strelko V.V. Sorption characteristics of "food fibers" in secondary products of processing of vegetable raw materials. *Russian Journal of Applied Chemistry*. 2001. **74**(4): 592.
36. Gun'ko V.M., Turov V.V., Krupska T.V., Pakhlov E.M. Behavior of water and methane bound to hydrophilic and hydrophobic nanosilicas and their mixture. *Chemical Physics Letters*. 2017. **690**: 25.
37. Zakutevskii O.I., Psareva T.S., Strelko V.V., Kartel' N.T. Sorption of U(VI) from aqueous solutions with carbon sorbents. *Radiochemistry*. 2007. **49**(1): 67.
38. Protsak I., Gun'ko V.M., Turov V.V., Krupska T.V., Pakhlov E.M., Zhang D., Dong W., Le Z. Nanostructured polymethylsiloxane/fumed silica blends. *Materials*. 2019. **12**(15): 2409.
39. Kartel M., Galysh V. New composite sorbents for caesium and strontium ions sorption. *Chemistry Journal of Moldova*. 2017. **12**(1): 37.
40. Gun'ko V.M., Turov V.V., Protsak I.S., Krupska T.V., Pakhlov E.M., Tsapko M.D. Effects of pre-adsorbed water on methane adsorption onto blends with hydrophobic and hydrophilic nanosilicas. *Colloids and Surfaces A: Physicochemical and Engineering Aspects*. 2019. **570**: 47.
41. Galysh V., Sevastyanova O., Kartel M., Lindström M.E., Gornikov Y. Impact of ferrocyanide salts on the thermo-oxidative degradation of lignocellulosic sorbents. *Journal of Thermal Analysis and Calorimetry*. 2017. **128**(2):1019.

42. Turov V.V., Gun'ko V.M., Krupska T.V., Borysenko M.V., Kartel M.T. Interfacial behavior of polar and nonpolar frozen/unfrozen liquids interacting with hydrophilic and hydrophobic nanosilicas alone and in blends. *Journal of Colloid and Interface Science*. 2021. **588**: 70.
43. Gabdullin M.T., Khamitova K.K., Ismailov D.V., Sultangazina M.N., Kerimbekov D.S., Yegemova S.S., Chernoshtan A., Schur D.V. Use of nanostructured materials for the sorption of heavy metals ions. *IOP Conference Series: Materials Science and Engineering*. 2019. **511**(1): 12044.
44. Savenko A.F., Bogolepov V.A., Meleshevich K.A., Zaginaichenko S.Yu., Lototsky M.V., Pishuk V.K., Teslenko L.O., Skorokhod V.V. Structural and methodical features of the installation for the investigations of hydrogen-sorption characteristics of carbon nanomaterials and their composites. *NATO Security through Science Series A: Chemistry and Biology*. 2007: 365.
45. Zaginaichenko S., Nejat Veziroglu T. Peculiarities of hydrogenation of pentatomic carbon molecules in the frame of fullerene molecule C_{60}. *International Journal of Hydrogen Energy*. 2008. **33**(13): 3330 .
46. Zaginaichenko S.Yu., Veziroglu T.N., Lototsky M.V., Bogolepov V.A., Savenko A.F. Experimental set-up for investigations of hydrogen-sorption characteristics of carbon nanomaterials. *International Journal of Hydrogen Energy*. 2016. **41**(1): 401.
47. Lakhnik A.M., Kirian I.M., Rud A.D. The Mg/MAX-phase composite for hydrogen storage. International Journal of Hydrogen Energy. 2022. **47**(11): 7274.
48. Schur D.V., Zaginaichenko S.Y., Savenko A.F., Bogolepov V.A., Anikina N.S., Zolotarenko, A.D., Matysina, Z.A., Veziroglu, T.N., Skryabina, N.E. Hydrogenation of fullerite C_{60} in gaseous phase. *NATO Science for Peace and Security Series C: Environmental Security*. 2011. **2**: 87.
49. Bogolepov, V.A., Veziroglu, A., Zaginaichenko, S.Y., Savenko A.F., Meleshevich K.A. Selection of the hydrogen-sorbing material for hydrogen accumulators. International Journal of Hydrogen Energy. 2016. **41**(3): 1811.
50. Shchur D.V., Zaginaichenko S.Y., Veziroglu A., Veziroglu T.N., Gavrylyuk N.A., Zolotarenko A.D., Gabdullin M.T., Ramazanov T.S., Zolotarenko A.D., Zolotarenko A.D. Prospects of Producing Hydrogen-Ammonia Fuel Based on Lithium Aluminum Amide. *Russian Physics Journal*. 2021. **64**(1): 89.
51. Matysina Z.A. Phase transformations $\alpha \rightarrow \beta \rightarrow \gamma \rightarrow \delta \rightarrow \varepsilon$ in titanium hydride tihx with increase in hydrogen concentration. *Russian Physics Journal.* 2001. **44**(11): 1237.
52. Trefilov V.I., Pishuk V.K., Zaginaichenko S.Yu., Choba A.V., Nagornaya N.R. Solar furnaces for scientific and technological investigation. *Renewable energy*. 1999. **16**(1-4): 757.
53. Lyashenko A.A., Adejev V.M., Voitovich V.B., Zaginaichenko S.Yu. Niobium as a construction material for a hydrogen energy system. *International Journal of Hydrogen Energy*. 1995. **20**(5): 405.
54. Lavrenko V.A., Adejev V.M., Kirjakova I.E. Studies of the hydride formation mechanism in metals. *International Journal of Hydrogen Energy*. 994. **19**(3): 265.
55. Matysina Z.A., Gavrylyuk N.A., Kartel M., Veziroglu A., Veziroglu T.N., Pomytkin A.P., Schur D.V., Ramazanov T.S., Gabdullin M.T., Zolotarenko A.D., Zolotarenko A.D., Shvachko N.A. Hydrogen sorption properties of new magnesium intermetallic compounds with $MgSnCu_4$ type structure. *International Journal of Hydrogen Energy*. 2021. **46**(50): 25520.
56. Matysina Z.A., Pogorelova O.S., Zaginaichenko S.Yu. The surface energy of crystalline CuZn and FeAl alloys. *Journal of Physics and Chemistry of Solids.* 1995. **56**(1): 9.

57. Rud A.D., Schmidt U., Zelinska, G.M., Lakhnik, A.M., Kolbasov G.Ya., Danilov M.O. Atomic structure and hydrogen storage properties of amorphous-quasicrystalline Zr-Cu-Ni-Al melt-spun ribbons. *Journal of Non-Crystalline Solids*. 2007. **353**(32-40): 3434.
58. Matysina Z.A., Zaginaichenko S.Yu. Hydrogen solubility in alloys under pressure. International *Journal of Hydrogen Energy*. 1996. **21**(11-12): 1085.
59. Zaginaichenko S.Yu., Matysina Z.A., Smityukh I., Pishuk V.K. Hydrogen in lanthan-nickel storage alloys. *Journal of Alloys and Compounds*. 2002. **330-332**: 70.
60. Lytvynenko Yu.M., Utilization the concentrated solar energy for process of deformation of sheet metal. *Renewable Energy*. 1999. **16**(1-4): 753.
61. Matysina Z.A., Zaginaichenko, S.Y. Sorption Properties of Iron–Magnesium and Nickel–Magnesium Mg_2FeH_6 and Mg_2NiH_4 Hydrides. *Russian Physics Journal*. 2016. **59**(2): 177.
62. Rud A.D., Schmidt U., Zelinska G.M., Lakhnik A.M., Perekos A.E., Kolbasov G.Ya., Danilov M.O. Peculiarities of structural state and hydrogen storage properties of Ti-Zr-Ni based intermetallic compounds. *Journal of Alloys and Compounds*. 2005. **404-406**: 515.
63. Zaginaichenko S.Y., Matysina Z.A., Teslenko L.O., Veziroglu A. The structural vacancies in palladium hydride. Phase diagram. *International Journal of Hydrogen Energy*. 2011. **36(**1): 1152.
64. Zaginaichenko S.Y., Zaritskii D.A., Matysina Z.A., Veziroglu T.N., Kopylova L.I. Theoretical study of hydrogen-sorption properties of lithium and magnesium borocarbides. *International Journal of Hydrogen Energy*. 2015. **40**(24): 7644.
65. Matysina Z.A., Zaginaichenko S.Y. Hydrogen-sorption properties of magnesium and its intermetallics with Ca7Ge-Type structure. *Physics of Metals and Metallography*. 2013. **114**(4): 308.
66. Tikhotskii S.A, Fokin I.V. Traveltime seismic tomography with adaptive wavelet parameterization. *Izvestiya. Physics of the Solid Earth*. 2011. **47**(4): 327.
67. Pylypova O., Havryliuk O., Antonin S., Evtukh A., Skryshevsky V., Ivanov I., Shmahlii S. Influence of nanostructure geometry on light trapping in solar cells. *Applied Nanoscience*. 2022. **12**(3): 769.
68. Semchuk O.Y., Biliuk A.A., Havryliuk O.O., Biliuk A.I. Kinetic theory of electroconductivity of metal nanoparticles in the condition of surface plasmon resonance. *Applied Surface Science Advances*. 2021. **3**: 100057.
69. Havryliuk O.O., Evtukh A.A., Pylypova O.V., Semchuk O.Y., Ivanov I.I., Zabolotnyi V.F. Plasmonic enhancement of light to improve the parameters of solar cells. *Applied Nanoscience*. 2020. **10**(12): 4759.
70. Tkachenko S., Brodnikovskyi D., Cizek J. Komarov P., Brodnikovskyi Ye., Tymoshenko Ya., Csaki S., Pinchuk M., Vasylyev O., Čelko L., Gadzyra M., Chraska T. Novel Ti–Si–C composites for SOFC interconnect materials: Production optimization. *Ceramics International*. 2022. **48**(19(A)): 27785.
71. Podhurska V., Brodnikovskyi D., Vasyliv B., Gadzyra M., Tkachenko S., Čelko L., Ostash O., Brodnikovska I., Brodnikovskyi Ye., Vasylyev O. *Ti-Si-C in-situ composite as a potencial material for lightweight SOFC interconnects. Promising materials and processes in applied electrochemistry* (Kyiv : KNUTD, 2020).
72. Brodnikovskyi Y., McDonald N., Polishko I., Brodnikovskyi D., Brodnikovska I., Brychevskyi M., Kovalenko L., Vasylyev O., Belous A., Steinberger-Wilckens R. Properties of 10Sc1CeSZ-3.5 YSZ (33-, 40-, 50-wt.%) composite ceramics for SOFC application. *Materials Today*. 2019. **6**: 26.
73. Polishko I., Ivanchenko S., Horda R., Brodnikovskyi Ye., Lysunenko N., Kovalenko L. Tape casted SOFC based on Ukrainian 8YSZ powder. *Materials Today*. 2019. **6**(2): 237.
74. Ilyin A.P., Mostovshchikov A.V., Root, L.O., Zmanovskiy S.V., Ismailov D.V., Ruzieva G.U. Effect of beta-radiation exposure on the parameters of aluminum micropowders

activity. Bulletin of the Tomsk Polytechnic University, Geo Assets Engineering. 2019. **330**(8): 87.
75. Karachevtseva L., Kartel M., Kladko V., Gudymenko O., Bo W., Bratus V., Lytvynenko O., Onyshchenko V., Stronska O. Functionalization of 2D macroporous silicon under the high-pressure oxidation. *Applied Surface Science*. 2018. **434**: 142.
76. Brodnikovska I., Brychevskyia M., Brodnikovskyi Y., Brodnikovskyi D., Vasylyev O., Smirnova A. Joint impedance spectroscopy and fractography data analysis of ceria doped scandia stabilized zirconia solid electrolyte modified by powder types and sintering temperature. *French-Ukrainian Journal of Chemistry*. 2018. **6**(1): 128.
77. Baglyuk G.A., Poznyak L.A. The sintering of powder metallurgy high-speed steel with activating additions. *Powder Metallurgy and Metal Ceramics*. 2002. **41**(7-8): 366.
78. Brodnikovsky D.N., Golovash A.V., Tkachenko S.V., Okun I.Yu., Kuz'menko N.N., Firstov S.A. Influence of rigid particles of silicide on character of deformation of alloys on the base of a titanium at the high temperatures. *Metallofizika i noveishie tekhnologii*. 2006. **28**: 165.
79. Baglyuk G.A., Poznyak L.A. Sintered wear-resistant iron-based materials. I. Materials fabricated by sintering and impregnation. *Poroshkovaya Metallurgiya*. 2001. (1-2): 44.
80. Baglyuk G.A., Ivasyshyn O.M., Stasyuk O.O., Savvakin D.G. Sintered metals and alloys: The effect of charge component composition on the structure and properties of titanium matrix sintered composites with high-modulus compounds. *Powder Metallurgy and Metal Ceramics*. 2017. **56**(1-2): 59.
81. Brodnikovskii D.N., Lugovoi N.I., Brodnikovskii N.P., Slyunyaev V.N., Kuz'menko N.N., Vasil'ev A.D., Firstov S.A. Powder metallurgy production of Ti–5.4 wt.% Si Alloy. II. Structure and Strength of the Sintered Material. *Powder Metallurgy and Metal Ceramics*. 2014. **52**: 539.
82. Abdullin K.A., Gabdullin M.T., Gritsenko L.V., Ismailov D.V., Kalkozova Z.K., Kumekov S.E., Mukash Z.O., Sazonov A.Y., Terukov E.I. Electrical, optical, and photoluminescence properties of ZnO films subjected to thermal annealing and treatment in hydrogen plasma. *Semiconductors*. 2016. **50**(8): 1010.
83. Baglyuk G.A., Sosnovskii L.A., Volfman V.I. Effect of carbon content on the properties of sintered steels doped with manganese and copper. *Powder Metallurgy and Metal Ceramics*. 2011. **50**(3-4): 189.
84. Matvienko Y., Rud A., Polishchuk S., Zagorodniy Y., Rud N., Trachevski V. Effect of graphite additives on solid-state reactions in eutectic Al–Cu powder mixtures during high-energy ball milling. *Applied Nanoscience*. 2020. **10**(8): 2803.
85. Baglyuk G.A., Tolochin A.I., Tolochina A.V., Yakovenko R.V., Gripachevckii A.N., Golovkova M.E. Effect of Process Conditions on the Structure and Properties of the Hot-Forged Fe_3Al Intermetallic Alloy. *Powder Metallurgy and Metal Ceramics*. 2016. **55**(5-6): 297.
86. Havryliuk O.O., Semchuk O.Y. Formation of periodic structures on the solid surface under laser irradiation. *Ukrainian Journal of Physics*. 2017. **62**(1): 20.
87. Khomenko E.V., Baglyuk G.A., Minakova R.V. Effect of deformation processing on the properties of Cu-50% Cr composite. *Powder Metallurgy and Metal Ceramics*. 2009. 48(3-4): 211.
88. Mostovshchikov A.V., Ilyin A.P., Zabrodina I.K., Root L.O., Ismailov D.V. Measuring the changes in copper nanopowder conductivity during heating as a method for diagnosing its thermal stability. *Key Engineering Materials*. 2018. **769**: 146.
89. Sizonenko O.N., Baglyuk G.A., Taftai E.I., Zaichenko A.D., Lipyan E.V., Torpakov A.S., Zhdanov A.A., Pristash N.S. Dispersion and carburization of titanium powders by electric discharge. *Powder Metallurgy and Metal Ceramics.* 2013. **52**(5-6): 247.

90. Semchuk O.Y., Biliuk A.A., Havryliuk O.O. The Kinetic Theory of the Width of Surface Plasmon Resonance Line in Metal Nanoparticles. *Springer Proceedings in Physics*. 2021. **264**: 3.
91. Brodnikovskii D.N., Lugovoi N.I., Brodnikovskii N.P., Slyunyaev V.N., Kulak L.D., Vasil'ev A.D., Firstov S.A. Powder metallurgy production of Ti–5.4 wt.% Si alloy. I. Simulating the formation of powder particles by centrifugal atomization. *Powder Metallurgy and Metal Ceramics*. 2013. **52**: 409.
92. Biliuk A.A., Semchuk O.Y., Havryliuk O.O. Kinetic theory of absorption of ultrashort laser pulses by ensembles of metallic nanoparticles under conditions of surface plasmon resonance. *Himia, Fizika ta Tehnologia Poverhni*. 2022. **13**(2): 556.
93. Baglyuk G.A., Napara-Volgina S.G., Vol'Fman V.I., Mamonova A.A., Pyatachuk S.G. Thermal synthesis of Fe-B 4C powder master alloys. *Powder Metallurgy and Metal Ceramics*. 2009. **48**(7-8): 381.
94. Gun'ko V.M., Turov V.V., Pakhlov E.M., Matkovsky A.K., Krupska T.V., Kartel M.T., Charmas B. Blends of amorphous/crystalline nanoalumina and hydrophobic amorphous nanosilica. *Journal of Non-Crystalline Solids*. 2018. **500**: 351.
95. Brodnikovska I., Khomenkova L., Korsunska N., Polishchuk Yu., Brychevskyi M., Brodnikovskyi Ye., Brodnikovskyi D., Polishko I., Vasylyev O. The investigation of 10Sc1CeSZ structure transformation and ionic conductivity. *Materials Today: Proceedings*. 2022. **50**(1): 487.
96. Biliuk A.A., Semchuk O.Y., Havryliuk O.O. Width of the surface plasmon resonance line in spherical metal nanoparticles. *Semiconductor Physics, Quantum Electronics and Optoelectronics*. 2020. **23**(3): 308.
97. Baglyuk G.A., Terekhov V.N., Ternovoi Y.F. Structure and properties of powder austenitic die steels. *Powder Metallurgy and Metal Ceramics*. 2006. **45**(7-8): 317.
98. Brodnikovska I., Korsunska N., Khomenkova L., Polishchuk Yu., Lavoryk S, Brychevskyi M., Brodnikovskyi Y., Vasylyev O. Grains, grain boundaries and total ionic conductivity of 10Sc1CeSZ and 8YSZ solid electrolytes affected by crystalline structure and dopant content. *Materials Today: Proceedings*. 2019. **6**(2): 79.
99. Nastasiienko N., Palianytsia B., Kartel M., Larsson M., Kulik T. Thermal transformation of caffeic acid on the nanoceria surface studied by temperature programmed desorption mass-spectrometry, thermogravimetric analysis and ft–ir spectroscopy. *Colloids and Interfaces*. 2019. **3**(1): 34.
100. Tolochyn, O.I., Baglyuk, G.A., Tolochyna, O.V., Evych, Y.I., Podrezov, Y.M., Molchanovska, H.M. Structure and Physicomechanical Properties of the Fe_3Al Intermetallic Compound Obtained by Impact Hot Compaction. *Materials Science*. 2021. **56**(4): 499.
101. Busch G. Neue Seignette-Electrika. Helv. Phys. Acta. 1938. **11**: 269.
102. Hablützel J. Schweres Seignettesalz Dielectrische Untersuchungen an $KNaC_4H_2D_2O_6 \cdot 4D_2O$ – Kristallen. Ibid. 1938. **11**: 489.
103. Mason W.P. A Dynamic Measurement of the Elastic, Electric and Piezoelectric Constans of Rochelle salt. *Phys. Rev.* 1939. **55**: 775.
104. Bantle W. Die spezifische wärme seignette-electrischer substanzen. Dielectrische messungen an KD_2PO_4 – kristallen. *Helv. Phys. Acta.* 1942. **15**: 373.
105. Arx A., Bantle W. Polarisation und spezifische wärme von KH_2PO_4. *Helv. Phys. Acta.* 1943. **16**: 211.
106. Stephenson C.C., Hooly J.G. The heat capacity of potassium dihydrogen phosphate from 15 to 300^o K. The anomaly at the Curie temperature. *Am. Chem. Soc.* 1944. **66**: 1397.
107. Von Arx A., Bantle W. Der inverse piezoeffekt des seignette-elektrischen kristalls KH_2PO_4. *Helv. Phys. Acta*. 1944. **17**: 298.

108. Mason W.P. The elastic, piezoelectric and dielectric constants of potassium dihydrogen phosphate and ammonium dihydrogen phosphate. *Phys. Rev.* 1946. **69**: 73.
109. Zwicker B. Elastische untersuchungen an $NH_4H_2PO_4$ und KH_2PO_4. *Helv. Phys. Acta*. 1946. **19:** 523.
110. Beck M., Granicher H. Elektrooptische untersuchungen an kristallen der KH_2PO_4 – gruppe. *Helv. Phys. Acta*. 1950. **23**: 522.
111. Baumgartner H. Elektrische sättigungserscheinungen und elektro-kalorischer effekt von kaliumphosphat KH_2PO_4. *Helv. Phys. Acta*. 1950. **23**: 651.
112. Baumgartner H. Unterschied der dielektrizitätskonstanten zwischen einem freien und einem geklemmten KH_2PO_4 – kristall. *Helv. Phys. Acta*. 1951. **24**: 326.
113. Suemune Y. Thermal conductivity of the KH_2PO_4 – type single crystals. *J. Phys. Soc. Japan.* 1966. **21**(3-4): -802.
114. Suemune Y. Thermal conductivity of some ferroelectric crystals with hydrogen bonds. *J. Phys. Soc. Japan*. 1967. **22**(3). 735.
115. Strukov B.A., Amin M., Kopzik V.A. Comparative investigation of the specific heat of KH_2PO_4 (KDP) and KD_2PO_4 (DKDP) single crystals. *Phys. Stat. Sol.* 1968. **27**(2): 741.
116. Ramanaiah K.V., Varma K.B.P. Dispersion of photoelastic constants in doped KDP crystsls. *Bullettin of Matterials Science*. 1983. 5(2): 147.
117. Strukov B.A., Belov A.A. Thermal conductivity of ferroelastic crystals with an order-disorder phase transition on the example of KDP and DKDP. *Izv. Academy of Sciences of the USSR. Ser. Physical.* 1992. **56**(10): 40.
118. Korotkov L.N., Kravchenko S.A., Gridnev S.A., Fedosyuk R.M. Elastic and inelastic properties of mixed crystals of potassium-ammonium dihydrogen phosphate with a low content of ammonium. *Izv. Academy of Sciences of the USSR. Ser. Physical*. 1998. **62**(8): 1598.
119. Kenzig W. *Ferroelectrics and antiferroelectrics* (Moscow: IL, 1960)
120. Smolensky G.A., Bokov V.A., Isupov V.A., Krainik N.N., Pasynkov R.E., Shur M.S. *Ferroelectrics and antiferroelectrics* (L.: Nauka, 1971).
121. Smolensky G.A. (Ed.) *Physics of ferroelectric phenomena* (Moscow: Nauka, 1985).
122. Rudyak V.M. *Physical properties of ferroelectric crystals* (Kalinin: KSU, 1989).
123. Matycina Z.A. Investigation of the paraelectric-ferroelectric phase transition in KDP crystals.. *Izv. universities. Physics*. 2000. **9**: 112.
124. Matysina Z.A., Modlinsky M., Chumak V. Investigation of paraelectrician-ferroelectrician phase transition in KDP crystals. In: 4*th Int. Symp. "New Materials for Electrochemical Systems"*. (Canada, Montreal, 2001). P. 11.
125. Zaginaichenko S.Yu., Matysina Z.A., Schur D.V., Chumak V.A. Spontaneous polarization and its effect on physical characteristics of potassium, rubidium and cesium dehydrophosphates and arsenates. In: *Proceed. VII Int. Conf. "ICHMS`2001"*. (Alushta, Ukraine, 2001). 306.
126. West J. A quantitative X-ray analysis of the structure of potassium dihydrogen phosphate. *Krist*. 1930. **74**: 306.
127. Ubbelohde A.R., Woodward I. Structure and thermal properties associated with some hydrogen bondsin crystals. VII. Behaviour of KH_2PO_4 and KH_2AsO_4 on cooling. *Proc. Roy. Soc.* 1947. **188A**(25): 358.
128. Frazer B.C., Pepinsky R. X-ray analysis of the ferroelectric transition in KH_2PO_4. *Acta Cryst*. 1953. **6**: 273.
129. Barkla H.M., Finlayson D.M. The properties of KH_2PO_4 below the Curie point. *Phil. Mag.* 1953. **44**(7):109.
130. Bacon G.E., Pease R.S. A neutron diffraction study of potassium dihydrogen phosphate by fourier synthesis. *Proc. Roy. Soc.* 1953. **220A:** 397.

131. Peterson S.W., Levy H.A. Neutron diffraction study of tetragonal potassium dihydrogen phosphate. *J. Chem. Phys.* 1953. **21:** 2084.
132. Levy H.A., Peterson S.W., Simonsen S.H. Neutron diffraction study of the ferroelectric modification of potassium dihydrogen phosphate. *Phys. Rev.* 1954. **93:** 1120.
133. Bacon G.E., Pease R.S. A neutron-diffraction study of the ferroelectric transition of potassium dihydrogen phosphate. *Proc. Roy. Soc.* 1955. **230A:** 359.
134. Smirnov A.A. *Molecular-kinetic theory of metals* (Moscow: Nauka, 1966).

ПОРОШКИ КРИСТАЛІЧНОГО ДИГІДРОФОСФАТУ КАЛІЮ (KDP)

Ан.Д. Золотаренко [1,2], Ол.Д. Золотаренко [1,2], З.А. Матисіна[1], Н.А. Швачко [1,3], Н.Є. Аханова [4,5], М. Уалханова [5], Д.В. Щур [1,6], М.Т. Габдулін [4], Ю.І. Жирко [6], О.Д. Золотаренко [1], О.П. Рудакова [1,2], М.В. Чимбай [1,2], Ю.О. Тарасенко[2], О.О. Гаврилюк [2]

[1]Інститут проблем матеріалознавстваім. І.М. Францевича НАН України, вул. Кржижановського, 3, 03142 Київ, Україна
[2]Інститут хімії поверхні ім. О.О. Чуйка НАН України, вул. Генерала Наумова, 17, 03164 Київ, Україна
[1] Frantsevich Institute for Problems of Materials Science of N.A.S. of Ukraine, 3, Krzhizhanovskogo Str., 03142,Kyiv, Ukraine * A.D.Zolotarenko@gmail.com
[3] Київський національний університет будівництва і архітектури, проспект Повітрофлотський, 31, Київ, 03037, Україна.
[4] Казахстансько-Британський технічний університет (КБТУ) вул. Толе бі 59, Алмати, 050040 Казахстан.
[5] Національна нанотехнологічна лабораторіявідкритого типу, Казахський національний університет ім. Аль-Фарабі, пр. Аль-Фарабі, 71, Алмати, 050040 Казахстан.
[6]Інститут прикладної фізики НАН України, вул. Петропавлівська, 58, м. Суми, 40000, Україна.

Розглядається використання кристалів фероелектрика KDP (фосфати та арсенати калію, рубідію, цезію) та їх дейтерованих аналогів у різних галузях, у тому числі у створенні електрооптичних пристроїв та як поглинаючих водень. Описуються фізичні властивості KDP - кристалів, зміна їхніх властивостей поблизу температури фазового переходу, а також методи одержання нанокристалів KDP та їх застосування в біомедицині.

Також у роботі вказано: фазовий перехід у кристалах KDP, що відбувається близько кімнатної температури і виявляється у зміні їх фізичних властивостей, таких як діелектрична проникність, оптичні властивості та теплоємність. Крім того, наближення до температури фазового переходу викликає зміну параметрів гратки кристала, що може привести до появи аномальних ефектів.

Розглянута структура елементарної комірки дигідрофосфату калію (KH_2PO_4). Побудовані графіки температурної залежності параметру порядку спонтанної поляризації та графіки температурної залежності конфігураційної теплоємності кристала в області фазового переходу та побудовані графіки температурної залежності

зворотної та прямої діелектричної сприйнятливості. А також побудовані графіки параметру порядку, що характеризує ступінь спонтанної поляризації для різних температур, залежно від напруженості зовнішнього електричного поля.

Ключові слова: *KDP-кристали, термодинамічна теорія, фероелектрики, поглинаючі водень, молекулярно-кінетичні уявлення, порядок, закон Кюрі-Вейса.*